Journal of Peptide Science
J. Peptide Sci. 2006; **12**: 279–290
Published online 2 September 2005 in Wiley InterScience (www.interscience.wiley.com). DOI: 10.1002/psc.720

JOURNAL OF PEPTIDE SCIENCE

Detection of new amino acid sequences of alamethicins F30 by nonaqueous capillary electrophoresis–mass spectrometry

ARNDT PSUREK,[a] CHRISTIAN NEUSÜß,[b] THOMAS DEGENKOLB,[c] HANS BRÜCKNER,[c] ELVIRA BALAGUER,[d] DIANA IMHOF[e] and GERHARD K. E. SCRIBA[a]*

[a] University of Jena, School of Pharmacy, Department of Pharmaceutical Chemistry, Philosophenweg 14, D-07743 Jena, Germany
[b] Bruker Daltonik GmbH, Leipzig, Permoserstrasse 15, D-04318 Leipzig, Germany
[c] University of Giessen, Interdisciplinary Research Center, Department of Food Sciences, Heinrich-Buff-Ring 26-32, D-35392 Giessen, Germany
[d] University of Barcelona, Department of Analytical Chemistry, Av. Diagonal 647, 08028 Barcelona, Spain
[e] University of Jena, Department of Biochemistry, Philosophenweg 12, 07743 Jena, Germany

Received 19 May 2005; Accepted 25 July 2005

Abstract: The microheterogeneous alamethicin F30 (ALM F30) isolated from the fermentation of *Trichoderma viride* strain NRRL 3199 was analyzed by nonaqueous capillary electrophoresis coupled to electrospray ion-trap mass spectrometry (ESI-IT-MS) and electrospray time-of-flight mass spectrometry (ESI-TOF-MS). Tandem ESI-IT-MS was used for elucidation of the amino acid sequence based on the fragmentation pattern of selected parent ions. The MS/MS spectra using the $[M+3H]^{3+}$ or $[M+2H]^{2+}$ ions as precursor ions displayed the respective b- and the y-type fragments resulting from cleavage of the particularly labile Aib–Pro bond. The MS^3 of these fragments generated the b acylium ion series, as well as internal fragment ion series. Eleven amino acid sequences were identified, characterized by the exchange of Ala to Aib in position 6, Gln to Glu in positions 7 or 19 as well as the loss of the *C*-terminal amino alcohol. In addition, two truncated pyroglutamyl peptaibols were found. Overall, seven new sequences are reported compared to earlier LC–MS studies. The composition of the components was confirmed by on-line ESI-TOF-MS detection. Mass accuracy well below 5 ppm was observed. Quantification of the individual components was achieved by a combination of UV and TOF-MS detection. Copyright © 2005 European Peptide Society and John Wiley & Sons, Ltd.

Keywords: nonaqueous capillary electrophoresis; mass spectrometry detection; peptaibiotics; polypeptide antibiotics; peptaibols; alamethicin F30; α-aminoisobutyric acid; pyroglutamic acid

INTRODUCTION

Alamethicins are 20-residue peptaibol peptides isolated from the culture broth of the mold *Trichoderma viride* [1,2] exhibiting interesting physicochemical and biological activities, such as the formation of voltage-dependent ion channels in bilayer lipid membranes, as well as antibiotic activities [3]. The voltage-dependent ion channel formation by alamethicin can be described by the dipole flip-flop gating model of Boheim and Jung [4,5] based on electrical field–induced transbilayer orientational movements of single molecules. The conductance states of the ion conductivity pores vary with the number of parallelly arranged α-helices. Recently, single pore states could be stabilized by *C*-terminal conjugation of alamethicin with fullerene or a membrane-anchoring lipopeptide [6].

Peptaibols are linear peptides composed of 5–20 amino acids [7]. These compounds are exclusively biosynthesized by fungicolous, plant or entomopathogenic fungi, thus assuming potential importance in the parasitic life cycle of the producers [8]. The nonribosomal biosynthesis includes nonproteinogenic amino acids, in particular α-aminoisobutyric acid (Aib). Aib residues are conformationally restricted and favor the formation of 3_{10}- and α-helical structures. Peptaibols are amphiphilic because of the acylated, nonpolar *N*-terminus and the more polar, *C*-terminal amino alcohol. The name 'peptaibol' reflects the characteristics of this class of compounds being peptides containing Aib and a *C*-terminal amino alcohol.

Depending on the fermentation conditions, *T. viride* produces the neutral alamethicins F50 (ALM F50) or the acidic peptaibols alamethicins F30 (ALM F30) [2]. Both are microheterogeneous mixtures of closely related sequential analogs that possess a phenylalaninol (Pheol or Fol) at the *C*-terminus, while the *N*-terminus is acetylated. ALM F50 and ALM F30 differ in the amino acid in position 18, which is the (neutral) glutamine in the case of ALM F50 and the (acidic) glutamate residue in the case of ALM F30 [2,9]. The structure of ALM F30 has been confirmed by total synthesis [10].

Tandem mass spectrometry, especially electrospray ionization (ESI) or matrix-assisted laser desorption ionization (MALDI) coupled to quadrupole, ion-trap (IT) or time-of-flight (TOF) mass analyzers have been proven useful for structural studies of peptaibols [8]. The separation of the individual components of ALM F50 and ALM F30 has been achieved by reversed-phase high performance liquid chromotography (HPLC) and the structure of the components was determined

* Correspondence to: G. K. E. Scriba, School of Pharmacy, Department of Pharmaceutical Chemistry, University of Jena, Philosophenweg 14, 07743 Jena, Germany; e-mail: gerhard.scriba@uni-jena.de

by HPLC–ESI-MS^n by Brückner and coworkers [2]. The acidic ALM F30 and the neutral ALM F50 were isolated from the culture broth by XAD-2 column chromatography and separated by silica gel chromatography. The composition of the individual peptaibols was subsequently determined by HPLC–ESI-MS^n. According to this study, ALM F30 consists of two major components that differ in the amino acid in position 6 (Ala or Aib) and eight minor components.

Nonaqueous capillary electrophoresis (NACE) using solvents such as methanol, acetonitrile or *N*-methylformamide, instead of water, for the preparation of the background electrolytes is increasingly applied to analytical problems [11]. Important parameters such as efficiency and selectivity can be effectively modified when aqueous buffers are replaced by nonaqueous electrolyte solutions. Organic solvents favor interactions that are weak in aqueous media. Furthermore, the solubility and stability of many analytes and additives are enhanced in nonaqueous solvents. Moreover, nonaqueous solvents may be preferable for electrochemical detection as well as for electrospray ionization mass spectrometry (ESI-MS) detection [12].

Traditionally, peptides as hydrophilic compounds are analyzed by capillary electrophoresis (CE) using aqueous background electrolytes. However, beneficial effects of organic solvents for the separation of hydrophobic peptides in aqueous CE media have been described. For example, an acidic aqueous buffer containing 20% 2-propanol as organic modifier was applied to the analysis of isomeric *N*-palmitoylated bradykinin and *O*-palmitoylated gonadorelin as well as (cysteinyl-4,5)-palmitoylated peptide SP-C14 [13]. Hodges and coworkers described the separation of 18-residue α-helical amphipathic peptide diastereomers by capillary zone electrophoresis with highly concentrated (up to 400 mM) perfluorinated acid ion-pairing reagents in aqueous solution [14]. The authors attributed the successful separation to conformational changes between the peptide diastereomers and differences in hydrophobicity of the nonpolar face of the amphipathic α-helices and their interactions with the hydrophobic anionic ion-pairing reagent. On-line NACE–MS of hydrophobic peptides gramicidin S and bacitracin has been demonstrated [15]. The separations were achieved in an acetonitrile/methanol-based system containing ammonium acetate and formic acid. ESI-MS allowed the determination of three minor components in the case of gramicidin S and one minor component in the case of bacitracin. The current status of CE–MS for the analysis of proteins and peptides including NACE–MS has been recently summarized [16].

The separation of peptaibols by CE has not been described previously. However, because of their lipophilic nature, NACE seems to be a suitable electromigration technique for this class of compounds. Thus, the present study was conducted in order to evaluate the potential of NACE coupled to MS for the analysis of peptaibols including the determination of their amino acid sequence. The natural ALM F30 was selected as model peptaibols because these compounds contain a glutamic acid residue in position 18 that can be deprotonated for electrophoretic analysis.

MATERIALS AND METHODS

Chemicals

Methanol, acetonitrile, 2-propanol, dichloromethane (all HPLC grade quality), ammonium acetate and silica gel 60 (mesh size <0.063 mm) were purchased from VWR International (Darmstadt, Germany). Ammonium formate was obtained from Sigma-Aldrich (Steinheim, Germany). Ammonium acetate and ammonium formate were dried overnight in a desiccator over silica before use. ALM F30 was isolated from fermentations of *T. viride* strain NRRL 3199 as described previously [2].

The peptides Pyr-Aib-Val-Aib-Gly-Leuol and Glu-Aib-Val-Aib-Gly-Leuol were synthesized by solid-phase synthesis using the Fmoc strategy for the assembly of the peptide on the solid support [17,18]. The Fmoc-protected terminating amino alcohol was directly anchored onto the 2-chlorotrityl chloride resin. Activation of the sterically hindered Aib was achieved using tetramethylfluoroformamidinium hexafluorophosphate (TFFH) as coupling reagent, as described by Carpino *et al.* [18]. The peptides were purified by preparative HPLC, and their identity was confirmed by MALDI-MS.

Capillary electrophoresis

CE with UV detection was performed on a Beckman P/ACE 5510 instrument (Beckman Coulter, Krefeld, Germany) equipped with a diode-array detector at 25 °C using 50-μm i.d. fused-silica capillaries (Polymicro Technologies, Phoenix, AZ, USA) with an effective length of 50 cm and a total length of 57 cm. UV detection was carried out at 215 nm at the cathodic end of the capillary. Sample solutions were introduced at the anodic end by hydrodynamic injections at a pressure of 0.5 psi for 3 s.

CE–MS experiments were performed using a Hewlett Packard ^{3D}CE instrument (Agilent Technologies, Waldbronn, Germany). Separations were performed at 25 °C in 50-μm i.d. fused-silica capillaries with a length of 57 cm by application of a separation voltage of 30 kV (sprayer grounded). A pressure of 50 mbar for 4 s was used for sample injection.

New capillaries were rinsed for 30 min with 0.1 M sodium hydroxide, 5 min with water and 10 min with methanol followed by the separation medium for 10 min. Between analyses, the capillary was flushed with the running buffer for 2 min. When not in use, it was washed with the respective solvent and then stored under dry conditions.

Electrospray Ionization Mass Spectrometry

On-line coupling of the CE instrument to the mass spectrometer detector was achieved with an Agilent coaxial sheath-liquid sprayer interface (Agilent Technologies, Palo Alto, CA, USA). The sheath liquid, 2-propanol : water (1 : 1, v/v) containing 1% formic acid, was supplied at a flow rate of 4 μl/min by a

syringe pump (Cole-Palmer, Vernon Hill, IL, USA). Nebulizer gas pressure was set to 2–3 psi. All ESI-MS experiments were carried out in positive ionization mode at 4500 V.

ESI-IT-MS measurements were performed using an ion-trap mass spectrometer Esquire HCT™ (Bruker Daltonik, Bremen, Germany). Mass spectra were acquired from m/z 200 to 1500 in the scanning mode and automatic switching between MS and MS^n. Ions were scanned at a speed of 8300 m/z per s in the MS mode in order to achieve sufficient resolution for charge attribution of triply charged peptides. The enhanced auto-MS^n settings were optimized to get as many MS^n spectra over a selected time period as possible. This was achieved by scanning at 26 000 m/z per s and active exclusion after two spectra per mass in a given time window of 0.5 min. MS^2 and MS^3 spectra were acquired selecting one (MS^2) or two (MS^3) most abundant precursors or by adding preferred masses in the case of follow-up experiments.

ESI-TOF-MS measurements were performed on an orthogonal TOF mass spectrometer micrOTOF™ (Bruker Daltonik, Bremen, Germany). The mass spectrometer operated in an m/z range 200–1500.

Data processing was performed by DataAnalysis™ software (Version 3.0; Bruker Daltonik). The peptide MS fragments are labeled according to standard rules [19,20].

RESULTS AND DISCUSSION

NACE Separation of ALM F30

NACE separation of the microheterogeneous ALM F30 was evaluated in methanol, acetonitrile and mixtures of these solvents using ammonium acetate– and ammonium formate–based electrolytes. The solvents are widely used in NACE because of their appropriate dielectric constant–to-viscosity ratio [11]. While electrolyte solutions in acetonitrile and acetonitrile–methanol mixtures did not afford satisfactory separations because of the low mobility of the analytes in these solvents, good separation selectivity was obtained using methanol-based electrolytes. 12.5 mM ammonium formate in methanol yielded six separated peaks using UV detection (data not shown).

Subsequent NACE–ESI-MS was performed using this background electrolyte and a sheath liquid consisting of 1% formic acid in a 1 : 1 mixture of 1-propanol and water, which provided stable spray and protonation conditions for the peptaibols. Figure 1 shows the base peak electropherogram of

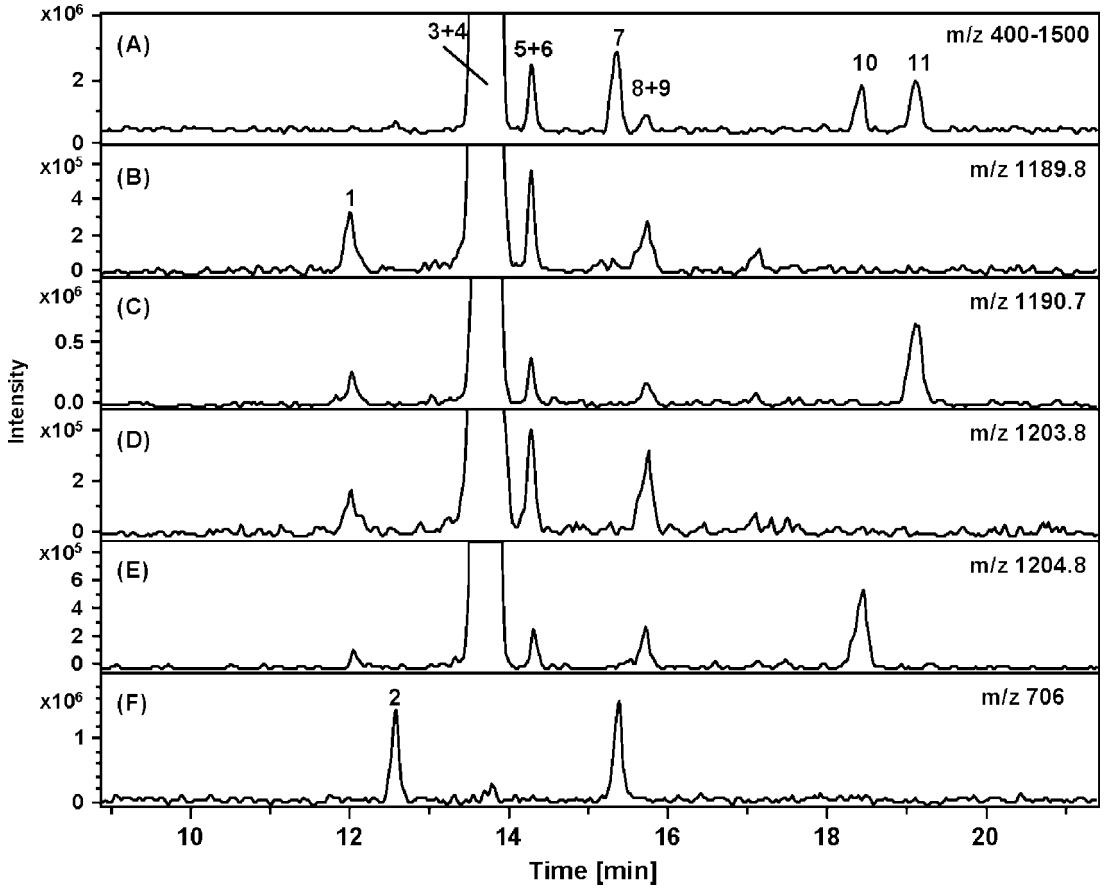

Figure 1 Extracted ion electropherograms of NACE with full-scan ESI-IT-MS detection. (A) Base peak electropherogram. (B–E) Mass traces of the different b_{13} fragments (see Table 2). (F) $[M + 2H]^{2+}$ pseudomolecular ion of the Pyr-containing peptides. Experimental conditions: capillary dimensions, 57 cm × 50 μm i.d.; running electrolyte, 12.5 mM ammonium formate in methanol; separation voltage, 30 kV (18 μA); for ESI-MS conditions see Experimental Section. Sample concentration: 500 μg/ml in methanol. Peak identity: numbers refer to peptide sequences shown in Table 1.

ALM F30 (Figure 1A) as well as electropherograms of selected mass traces of the characteristic b_{13} fragment ions obtained with full-scan ESI-IT-MS (Figure 1B–E). The identification of the individual components and the determination of their amino acid sequences are discussed below. The extracted ion electropherogram (EIE) of the b_{13} fragments at *m/z* 1189.9 (Figure 1B) and 1203.8 (Figure 1D) as well as at *m/z* 1190.7 (Figure 1C) and 1204.8 (Figure 1E) with mass differences of 14 Da correspond to the exchange of Ala by Aib in the peptaibols. Most of the respective compounds comigrated, as the mass difference of 14 Da is apparently not large enough to be translated into electrophoretic separations of otherwise identical peptaibols with molecular masses of about 1900–1950 Da. The EIE of *m/z* 706 (Figure 1F) corresponds to the doubly charged pseudomolecular $[M + 2H]^{2+}$ ions of truncated pyroglutamyl (Pyr) peptaibols.

Amino Acid Sequence Determination

Table 1 summarizes the amino acid sequences of ALM F30 as determined by NACE–ESI-MS analysis. A different numbering as compared to the nomenclature applied in Ref. 2 of the ALM F30 peptides is used for reasons of simplicity. The mass fragments and molecular ions of all components of ALM F30 determined in this study are compiled in Table 2. The majority of the diagnostic ions was identified via NACE–ESI-IT-MS^n in the positive ion mode from specific precursor ions such as the triply and doubly charged pseudomolecular $[M + 3H]^{3+}$ and $[M + 2H]^{2+}$ ions for MS^2 spectra and from the b_{13} and y_7 fragments, respectively, in the case of the MS^3 spectra. Figures 2 and 3 show the ESI-IT-MS^3 spectra of [Aib^6] ALM F30 (**3**) and [desAA(1–6),Pyr^7] ALM F30 (**7**), respectively, as examples.

The MS spectra show the doubly and triply charged pseudomolecular ions, $[M + 2H]^{2+}$ or $[M + 3H]^{3+}$, as well as the corresponding ammonium adducts in some cases. Moreover, b_{13}- and y_7-fragments are generated, resulting from fragmentation of the particularly labile Aib–Pro bond. The tertiary amide bond undergoes a preferential cleavage, leading to an *N*-terminal acylium ion (b-type fragment) and a diprotonated *C*-terminal ion (y-type fragment) [21]. These characteristic fragments were also obtained in the ESI-IT-MS full-scan mode (without MS^n) illustrating the facile cleavage of the Aib–Pro bond. Other peptaibols such as harzianins [21], stilboflavins [22], trichotoxins [23] and trichofumins [24] exhibit similar fragmentation patterns in ESI-MS. The MS^2 spectra using the $[M + 3H]^{3+}$ or $[M + 2H]^{2+}$ ions as precursor ions displayed the respective b- and the y-type fragments resulting from cleavage of the Aib–Pro bond. The selection of the appropriate precursor ions allowed the identification and amino acid sequence determination also in case of comigrating substances.

In the case of the 20- and 19-residue peptaibols, the triply charged pseudomolecular ions $[M + 3H]^{3+}$ were selected as the precursor ions for the MS^2 analysis

Table 1 Sequences and relative quantities (%) of the ALM F30 peptides characterized by NACE–ESI-MS in the microheterogeneous mixture. Exchanged amino acid positions are highlighted in bold letters. Abbreviations of the amino acids are according to the one-letter code, Ac – acetyl, U – Aib, Pyr – pyroglutamic acid. The denotation of the ALM F30 peptides identified by HPLC–MS [2] is listed in the third column

		Nomenclature in Ref. 2	%	1	2	3	4	5	6	7	8	9	10	11	12	13	14	15	16	17	18	19	20
1	ALM F50	F50/5	—[a]	Ac	U	P	U	A	U	A	Q	U	V	U	G	L	U	P	V	U	U	**Q**	Q	Fol
2	[desAA(1–6),Pyr^7] ALM F50	—	0.4							**Pyr**	U	V	U	G	L	U	P	V	U	U	**Q**	Q	Fol
3	[Aib^6] ALM F30	F30/7	38.9	Ac	U	P	U	A	U	U	Q	U	V	U	G	L	U	P	V	U	U	E	Q	Fol
4	ALM F30	F30/3	51.0	Ac	U	P	U	A	U	A	Q	U	V	U	G	L	U	P	V	U	U	E	Q	Fol
5	[Glu^{19}] ALM F30	—	1.4	Ac	U	P	U	A	U	A	Q	U	V	U	G	L	U	P	V	U	U	E	**E**	Fol
6	[Aib^6,Glu^{19}] ALM F30	—	1.2	Ac	U	P	U	A	U	**U**	Q	U	V	U	G	L	U	P	V	U	U	E	**E**	Fol
7	[desAA(1–6),Pyr^7] ALM F30	—	2.9							**Pyr**	U	V	U	G	L	U	P	V	U	U	E	Q	Fol
8	[desPheol] ALM F30	—	0.6	Ac	U	P	U	A	U	A	Q	U	V	U	G	L	U	P	V	U	U	E	Q	
9	[Aib^6,desPheol] ALM F30	—	0.7	Ac	U	P	U	A	U	**U**	Q	U	V	U	G	L	U	P	V	U	U	E	Q	
10	[Aib^6,Glu^7] ALM F30	—	1.3	Ac	U	P	U	A	U	**U**	**E**	U	V	U	G	L	U	P	V	U	U	E	Q	Fol
11	[Glu^7] ALM F30	F30/6	1.7	Ac	U	P	U	A	U	A	**E**	U	V	U	G	L	U	P	V	U	U	E	Q	Fol

[a] Not quantified, because the uncharged ALM F50 comigrates with the EOF.

Table 2 Fragment ions, pseudomolecular ions and adducts of pseudomolecular ions (m/z ratio) of ALM F30 determined by NACE–ESI-MS. The numbering of the components corresponds to Table 1

Diagnostic ion	m/z							Diagnostic ion	m/z		Diagnostic ion	m/z	
	1	**3**	**4**	**5**	**6**	**10**	**11**		**2**	**7**		**8**	**9**
b_2	225.1	225.1	225.1	225.1	225.1	225.1	225.1	b_2	n.d.	197.1	b_2	225.1	225.1
b_3	310.2	310.2	310.2	310.2	310.2	310.2	310.2	b_3	296.2	296.2	b_3	310.2	310.2
b_4	381.2	381.2	381.2	381.2	381.2	381.2	381.2	b_4	381.2	381.2	b_4	381.2	381.2
b_5	466.3	466.3	466.3	466.3	466.3	466.3	466.3	b_5	438.2	438.2	b_5	466.3	466.3
b_6	537.3	551.3	537.3	537.3	551.3	551.3	537.3	b_6	551.3	551.3	b_6	537.3	551.3
b_7	665.4	679.4	665.4	665.4	679.4	680.4	666.3	b_7	636.4	636.4	b_7	665.4	679.4
b_8	750.4	764.4	750.4	750.4	764.4	765.4	751.4	—	—	—	b_8	750.4	764.4
b_9	849.5	863.5	849.5	n.d.	n.d.	864.5	850.5	—	—	—	b_9	849.5	863.5
b_{10}	934.5	948.5	934.5	934.5	948.5	949.5	935.5	—	—	—	b_{10}	934.5	948.5
b_{13}	1189.7	1203.7	1189.7	1189.7	1203.7	1204.7	1190.7	—	—	—	b_{13}	1189.7	1203.7
$[b_{13} + 2H]^{2+}$	595.8	602.9	595.8	595.8	602.9	603.4	596.3	—	—	—	$[b_{13} + 2H]^{2+}$	595.8	602.9
y_7	774.4	775.4	775.4	776.4	776.4	775.4	775.4	y_7	774.4	775.4	y_6	642.3	642.3
$[y_7 - H_2O]$	756.4	757.4	757.4	758.4	758.4	757.4	757.4	$[y_7 - H_2O]$	756.4	757.4	$[y_6 - H_2O]$	624.3	624.3
y_7b_{19}	623.3	624.3	624.3	625.3	625.3	624.3	624.3	y_7b_{13}	623.3	624.3	—	—	—
y_7b_{18}	495.3	496.3	496.3	496.3	496.3	496.3	496.3	y_7b_{12}	495.3	496.3	y_6b_{18}	496.3	496.3
y_7b_{17}	367.2	367.2	367.2	367.2	367.2	367.2	367.2	y_7b_{11}	367.2	367.2	y_6b_{17}	367.2	367.2
y_7b_{16}	282.2	282.1	282.2	282.2	282.2	282.2	282.2	y_7b_{10}	282.2	282.2	y_6b_{16}	282.2	282.2
$b_{13}y_{10}$	256.2	256.2	n.d.	256.2	256.2	256.2	256.2	b_7y_{10}	256.2	256.2	$b_{13}y_9$	256.2	256.2
$b_{13}y_{11}$	341.2	341.2	341.2	341.2	341.2	341.2	341.2	$\underline{b}_7y_{11}$	341.2	341.2	$b_{13}y_{10}$	341.2	341.2
$b_{13}y_{12}$	440.3	440.3	440.3	440.3	440.3	440.3	440.3	b_7y_{12}	440.3	440.3	$b_{13}y_{11}$	440.3	440.3
$b_{13}y_{13}$	525.3	525.3	525.3	525.3	525.3	525.3	525.3	b_7y_{13}	525.3	525.3	$b_{13}y_{12}$	525.3	525.3
$b_{13}y_{14}$	653.4	653.4	653.4	653.4	653.4	654.4	654.4	—	—	—	$b_{13}y_{13}$	653.4	653.4
$b_{13}y_{15}$	724.4	738.4	724.4	724.4	738.4	739.4	725.4	—	—	—	$b_{13}y_{14}$	724.4	738.4
$b_{13}y_{16}$	809.5	823.5	809.5	809.5	823.5	824.5	810.5	—	—	—	$b_{13}y_{15}$	809.5	823.5
$b_{13}y_{17}$	880.5	894.5	880.5	880.5	894.5	895.5	881.5	—	—	—	$b_{13}y_{16}$	880.5	894.5
$[M + 2H]^{2+}$	982.1	989.6	982.6	983.1	990.1	990.0	983.1	$[M + 2H]^{2+}$	705.4	705.9	$[M + 2H]^{2+}$	916.0	923.0
$[M + NH_4 + H]^{2+}$	990.6	998.1	991.1	991.6	998.6	998.5	991.6	$[M + NH_4 + H]^{2+}$	713.9	714.4	$[M + NH_4 + H]^{2+}$	924.5	931.5
$[M + 3H]^{3+}$	655.1	660.1	655.4	655.7	660.4	660.4	655.7	$[M + 3H]^{3+}$	n.d.	n.d.	$[M + 3H]^{3+}$	611.0	615.7
$[M + NH_4 + 2H]^{3+}$	660.8	665.8	661.1	661.4	666.1	666.1	661.4	$[M + NH_4 + 2H]^{3+}$	n.d.	n.d.	$[M + NH_4 + 2H]^{3+}$	616.7	621.4

n.d. – not determined.

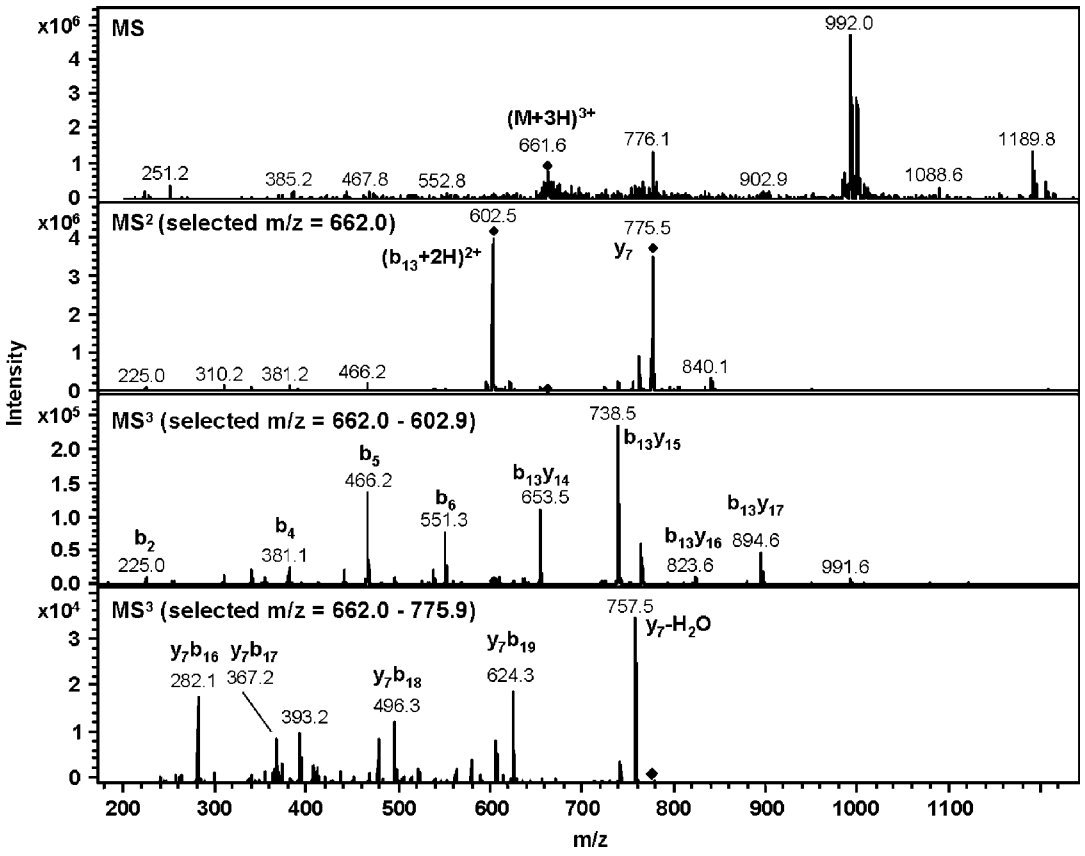

Figure 2 ESI-IT-MS^n ($n = 1–3$) of [Aib^6] ALM F30 (**3**).

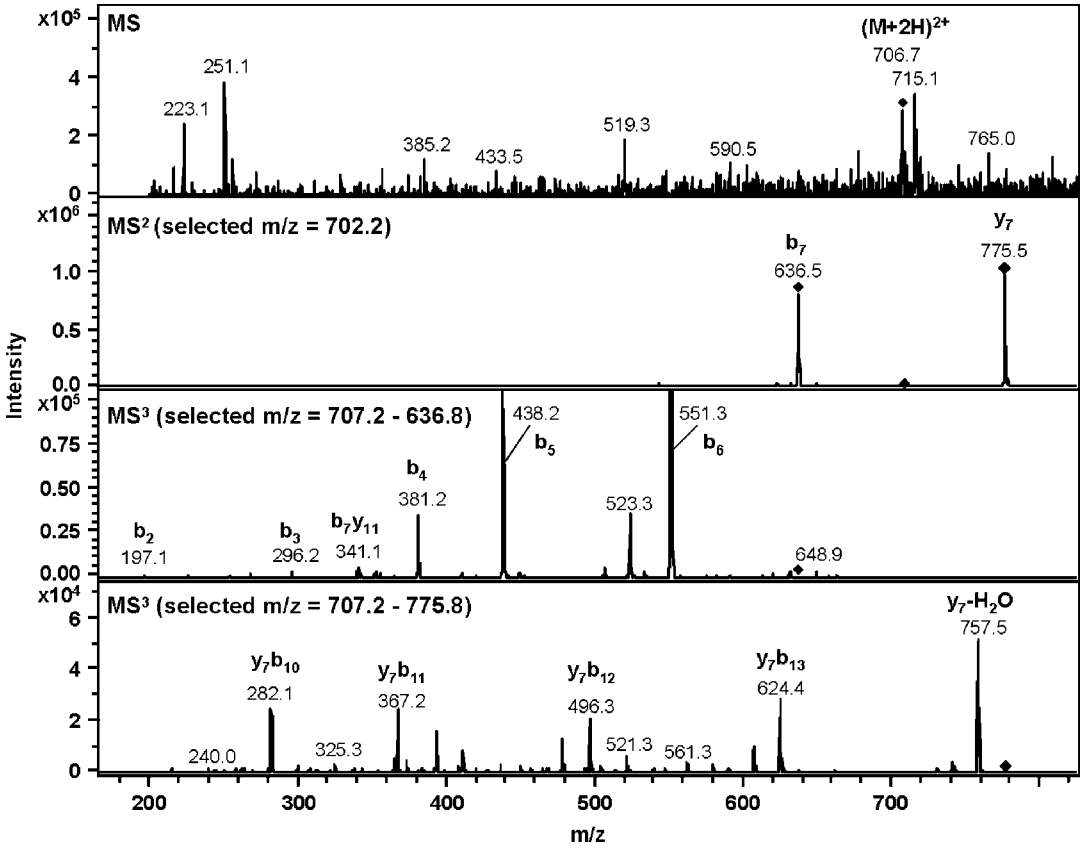

Figure 3 ESI-IT-MS^n ($n = 1–3$) of [desAA(1–6),Pyr^7] ALM F30 (**7**).

(Figure 2). MS^2 generated the b_{13} and the y_7 fragment or, in case of the desPheol ALM F30 peptides, the y_6 fragment (data not shown). The b_{13} fragment is detected as a doubly charged ion. The MS^3 of the diprotonated b_{13} fragment ($[b_{13} + 2H]^{2+}$) generated the $b_2 - b_{10}$ acylium ion series, as well as the monoprotonated internal fragments $b_{13}y_{10} - b_{13}y_{17}$ (Table 2). The *C*-terminal sequences of the peptides were determined by MS^3 of the y_7 fragment and, in the case of the desPheol ALM F30 peptides, of the y_6 fragment. The resulting internal ion series ($y_7b_{19} - y_7b_{16}$) are formed by the cleavage of *C*-terminal residues while the charge remains at the *N*-terminus. Loss of water from the y_7 fragment leads to a $y_7 - H_2O$ fragment ion in the MS^3 spectra. The *C*-terminal position of Pheol was concluded from the mass difference of 150 + 1 Da from diprotonated y_7 and monoprotonated y_7b_{19} fragments. A fragmentation scheme is presented in (Figure 4) showing the series of diagnostic ions and internal fragments used for sequence determination of [Aib^6] ALM F30 (**3**).

The signals of the b_2 ions were recorded at *m/z* 225 corresponding to the fragment Ac-Aib-Pro. The internal fragments $b_{13}y_{10}$ (*m/z* 256) and y_7b_{16} (*m/z* 282) correspond to the Gly-Leu-Aib and the Pro-Val-Aib tripeptides, respectively. The sequences of these three fragments were derived from earlier HPLC–MS investigations of ALM F30 [2,9] assuming sequence analogy.

The sequences of the two pyroglutamyl peptaibols (14-residue peptides) [desAA(1–6),Pyr^7] ALM F50 (**2**) and [desAA(1–6),Pyr^7] ALM F30 (**7**) were concluded from MS^3 analysis of the b_7 and y_7 fragments generated by the cleavage of the Aib-Pro bond of the pseudomolecular ion $[M + 2H]^{2+}$ (Figure 3 for [desAA(1–6),Pyr^7] ALM F30). The internal fragments of b_7 are the $b_2 - b_7$ acylium ion series and the monoprotonated fragments $b_7y_{10} - b_7y_{13}$ analogous to the b_{13} fragment of the 20-residue ALM F30 peptaibols. The y_7 fragment formed the $y_7b_{10} - y_7b_{13}$ internal fragment series. In contrast to the 20-residue ALM F30 peptides, the sequence of the b_7y_{10} fragment at *m/z* 256 corresponding to the Gly-Leu-Aib tripeptide could be confirmed by the $b_5 - b_7$ fragment ions.

Pandey *et al.* reported the formation of pyroglutamyl peptide fragments in an electron-impact mass spectrometry study of ALM F30 [9]. However, the formation of pyroglutamyl peptides during the ESI process has not been described. In order to evaluate the fragmentation pattern of Glu *versus* Pyr peptides, two model peptides containing reduced *C*-termini with the amino acid sequences Glu-Aib-Val-Aib-Gly-Leuol (Glu-hexapeptide) and Pyr-Aib-Val-Aib-Gly-Leuol (Pyr-hexapeptide) were synthesized and subjected to NACE–ESI-MS. The ESI-IT-MS^3 spectra of the two model hexapeptides displayed the respective b-type and the y-type ion series. The $[M + H]^+$ ions were selected as the precursor ions, and the fragment ions are listed in Table 3. In the spectrum of the Glu-hexapeptide, the b_2, b_3 and b_4 fragments were detected and also additional signals corresponding to the loss of water from the $b_2 - b_4$ fragments. These fragments have identical *m/z* values as the $b_2 - b_4$ fragments of the Pyr-hexapeptide so that formation of Pyr peptides in the ESI source can be assumed. However, the Glu-hexapeptide can be clearly distinguished by the presence of the $b_2 - b_5$ fragments 18 mass units higher than those of the Pyr-hexapeptide. In addition, both peptides have different electrophoretic mobilities. Thus, it can be concluded that the truncated Pyr peptaibol components in ALM F30 are in fact present in the investigated sample and not an artefact generated in the ESI ion source because the compounds did not display the respective 18-mass-units-higher fragments in the spectra. Interestingly, [desAA(1–6),Pyr^7] ALM F50 (**2**) displayed a low anodic mobility despite the fact that this compound should be neutral as it does not contain a charged amino acid. Apparently, under the present NACE conditions, a partial negative charge is induced. Moreover, the anodic mobility of [desAA(1–6),Pyr^7] ALM F50 (**2**)

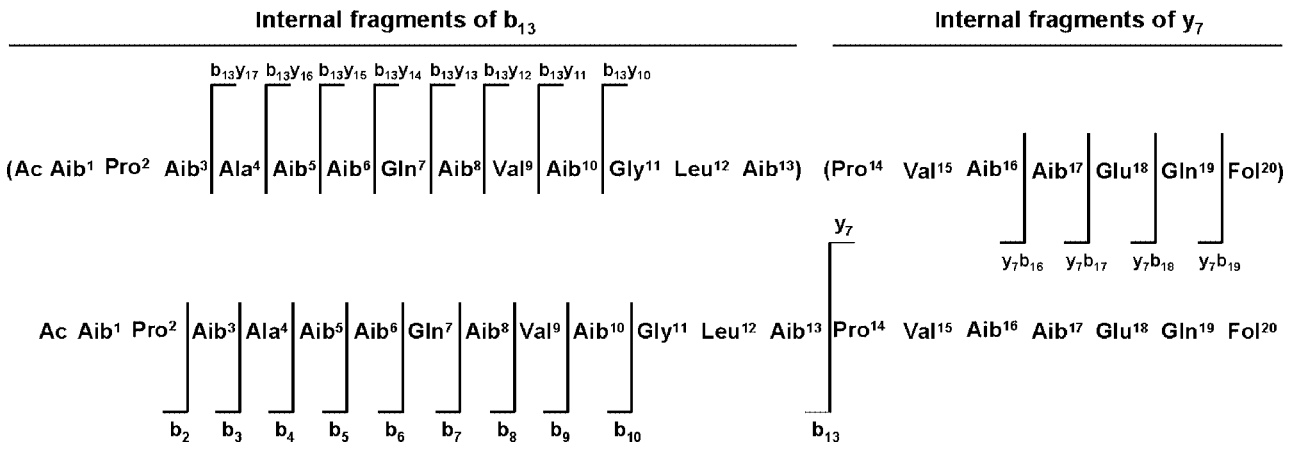

Figure 4 Fragmentation scheme of [Aib^6] ALM F30 (**3**). Fragments were generated by ESI-IT-MS^n ($n = 1–3$).

was confirmed by the anodic mobility of the Pyr model hexapeptide.

The amino acid composition of the ALM F30 components obtained by NACE–ESI-IT-MS^n was confirmed by NACE–ESI-TOF-MS analysis. Doubly or triply charged molecular ions were the most abundant ions in the spectra. Fragmentation was not observed (data not shown). The high resolution of the TOF mass analyzer allowed the analysis of the isotope pattern as shown in Figure 5 for the $[M + 3H]^{3+}$ ion of [desPheol] ALM F30 (**8**) and the $[M + 2H]^{2+}$ ion of [desAA(1–6),Pyr^7] ALM F30 (**7**) including a comparison of the experimental spectra with the simulated isotope pattern obtained by the Bruker DataAnalysis™ software. In both examples, the measured isotope pattern was consistent with the calculated isotope pattern, thus confirming the elemental composition, i.e. the amino acid composition of the identified components. This approach was applied to the confirmation of the amino acid composition of all compounds. Table 4 summarizes the experimentally determined monoisotopic m/z values using ALM F30 as mass calibrant compared to the respective calculated values. With the exception of the neutral ALM F50, mass accuracy was clearly below 5 ppm for the doubly charged ions and below 2 ppm for the triply charged ions. The relative inaccuracy found for ALM F50 may be due to the fact that this compound migrates essentially with the electroosmotic flow (EOF).

Table 3 Fragment ions, pseudomolecular ions and adducts of pseudomolecular ions (m/z ratio) of the model hexapeptides Glu-Aib-Val-Aib-Gly-Leuol (Glu-hexapeptide) and Pyr-Aib-Val-Aib-Gly-Leuol (Pyr-hexapeptide)

Ion	m/z	
	Glu-hexapeptide	Pyr-hexapeptide
b_2	215.1	197.1
b_3	314.2	296.2
b_4	399.2	381.2
b_5	456.2	438.2
y_2	157.1	157.1
y_3	242.2	242.2
y_4	341.2	341.2
y_5	426.3	426.3
$[b_2 - H_2O]$	197.1	—
$[b_3 - H_2O]$	296.2	—
$[b_4 - H_2O]$	381.2	—
$[M + H]^+$	573.3	555.3

Except for the neutral components ALM F50 (**1**) and [desAA(1–6),Pyr^7] ALM F50 (**2**), the compounds possess a Glu residue in position 18 and carry a negative charge under the applied NACE conditions. Not considering [desAA(1–6),Pyr^7] ALM F30 (**7**), the Glu^{18} derivatives can be divided into pairs characterized by the exchange of Ala by Aib in position 6. This exchange is characteristic for many peptaibol peptides [7]. Compared to the pair of the major components ALM F30 (**4**) and [Aib^6] ALM F30 (**3**), the other pairs are characterized by an additional carboxy group resulting from the exchange of Gln in position 19 to Glu, i.e. [Glu^{19}] ALM F30 (**5**) and [Aib^6,Glu^{19}] ALM F30 (**6**), the exchange of Gln to Glu in position 7, i.e. [Glu^7] ALM F30 (**11**) and [Aib^6,Glu^7] ALM F30 (**10**), or loss of the *C*-terminal phenylalaninol, i.e. [desPheol] ALM F30 (**8**) and [Aib^6,desPheol] ALM F30 (**9**). Except for [Glu^7] ALM F30 (**11**) and [Aib^6,Glu^7] ALM F30 (**10**), which are well separated, the peptaibols of the respective pairs comigrate as the mass difference of

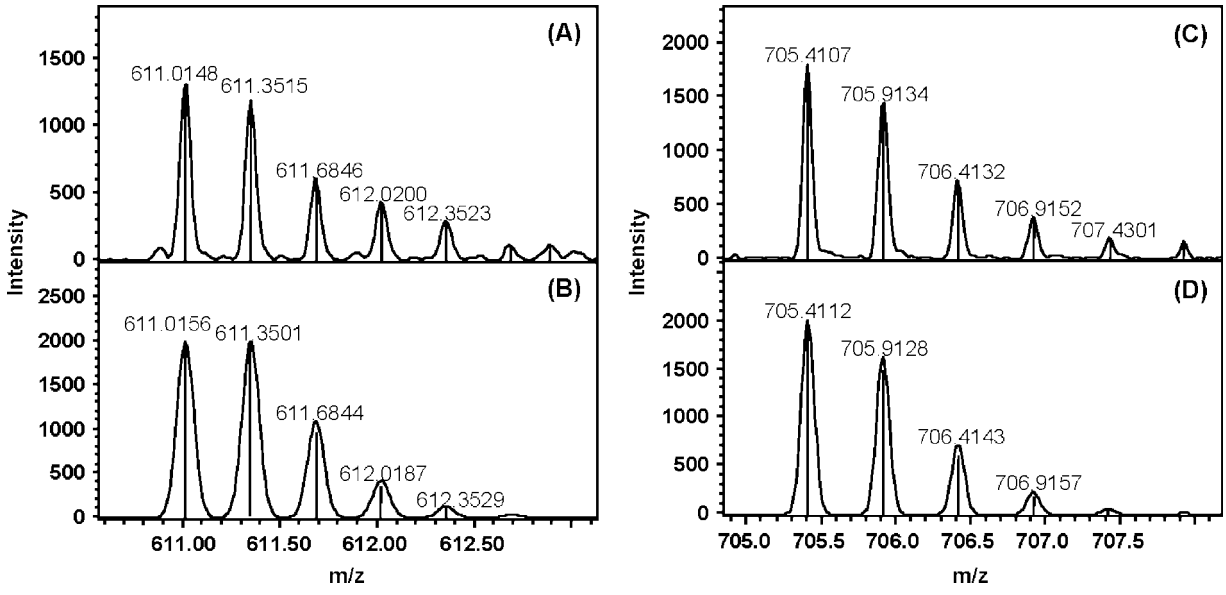

Figure 5 Measured (A, C) and calculated (B, D) isotope pattern of [desPheol] ALM F30 (A, B) and [desAA(1–6),Pyr^7] ALM F30 (C, D).

Table 4 Calculated and measured m/z ratios of the pseudomolecular ions observed in ESI-TOF-MS

		Molecular formula	Monoisotopic molecular mass (Da)	m/z monoisotopic mass					
				$[M+2H]^{2+}$		Δm (ppm)	$[M+3H]^{3+}$		Δm (ppm)
				Measured	Calculated		Measured	Calculated	
1	ALM F50	$C_{92}H_{151}N_{23}O_{24}$	1962.09	982.0784	982.0724	+6.1	655.0483	655.0507	−3.7
2	[des(1–6),Pyr^7] ALM F50	$C_{67}H_{108}N_{16}O_{17}$	1408.77	705.4107	705.4112	−0.7	—	—	—
3	[Aib^6] ALM F30	$C_{93}H_{152}N_{22}O_{25}$	1977.08	989.5723	989.5722	+0.1	660.0507	660.0506	+0.2
4	ALM F30	$C_{92}H_{150}N_{22}O_{25}$	1963.07	Calibrant	982.5644	—	Calibrant	655.3787	—
5	[Glu^{19}] ALM F30	$C_{92}H_{149}N_{21}O_{26}$	1964.05	983.0562	983.0564	−0.2	655.7075	655.7067	+1.2
6	[Aib^6,Glu^{19}] ALM F30	$C_{93}H_{151}N_{21}O_{26}$	1978.06	990.0609	990.0642	−3.3	660.3798	660.3786	+1.8
7	[des(1–6),Pyr^7] ALM F30	$C_{67}H_{107}N_{15}O_{18}$	1409.75	705.9031	705.9032	−0.1	—	—	—
8	[desPheol] ALM F30	$C_{83}H_{139}N_{21}O_{25}$	1830.00	916.0177	916.0198	−2.3	611.0148	611.0156	−1.3
9	[Aib^6,desPheol] ALM F30	$C_{84}H_{141}N_{21}O_{25}$	1844.01	923.0305	923.0276	+3.1	615.6873	615.6875	−0.3
10	[Aib^6,Glu^7] ALM F30	$C_{93}H_{151}N_{21}O_{26}$	1978.06	990.0634	990.0642	−0.8	660.3797	660.3786	+1.7
11	[Glu^7] ALM F30	$C_{92}H_{149}N_{21}O_{26}$	1964.05	983.0557	983.0564	−0.7	655.7066	655.7067	−0.2

14 Da caused by the exchange of Ala *versus* Aib is not sufficient to be translated into CE separations of peptaibols with masses of approximately 1950 Da under the experimental conditions applied.

Peptaibiotics terminating in a free amino acid or amide instead of a *C*-terminal 2-amino alcohol residue have been described previously. They comprise XR 586 (Gly at the *C*-terminus) [25]; trichobrachins TB I A, B, C, and D (Gln at the *C*-terminus) as well as trichobrachins II A, C, and D (Val at the *C*-terminus) [26]; lipohexin (β-Ala at the *C*-terminus) [27,28], pseudokonin KL III (Pro-NH_2 at the *C*-terminus) [29] and cephaibols P and Q (Ser at the *C*-terminus) [30].

N-terminal pyroglutamic acid (Pyr) containing peptaibols have not yet been reported. Whether [desAA(1–6),Pyr^7] ALM F50 (**2**) and [desAA(1–6),Pyr^7] ALM F30 (**7**) are naturally occurring compounds or artifacts caused by the workup or enzymatic degradation of peptaibols in the fermentation process remains to be answered. In order to estimate the possibility of the formation during workup, ALM F30 was heated for 41 h at 100 °C in the crystalline state as well as in dichloromethane/methanol (1 : 1, v/v) in the presence of an equal amount of silica gel G 60 for 4, 8 and 24 h at 70 °C in a closed vial simulating the chromatographic workup [2] of the sample. The samples were analyzed by LC–MS and CE. Neither treatment increased the amount of the truncated pyroglutamyl peptides compared to untreated samples. Thus, formation of these peptides during workup appears to be unlikely. In addition, when specifically searching for the mass trace of the [desAA(1–6),Pyr^7] ALM F30 (**7**) in LC–MS, the compound could also be detected in samples of ALM F30 described in Ref. 2.

To the best of our knowledge, this is the first report on the occurrence of Pyr as a constituent of fungal peptides in nature. Literature search did not reveal any previous publications regarding the isolation of peptide-bound Pyr from a fungal source. Pyr is rather widespread as an *N*-terminal constituent of peptides obtained from bacteria, plants, vertebrates and invertebrates. For example, the enzymatic production of Pyr by thermophilic lactic acid bacteria in Italian cheeses has been described [31,32]. Pyr has been reported as a constituent of antifungal peptides from the bark of *Eucommia ulmoides* [33], as a constituent of an adipokinetic hormone from the corpora cardiaca of the butterfly *Vanessa cardui* (Lepidoptera, Nymphalidae) [34], in gomesin, a defensive peptide found in the hemocytes of the tarantula spider *Acanthoscurria gomesiana* (Theraphosidae) [35], from the abdominal ganglia of the snail *Aplysia californica* [36], as well as from the hemolymph of the shrimp *Penaeus vannamei* (Decapoda) [37]. The *N*-terminus of neurotensins from the European green frog *Rana ridibunda* also contains a Pyr [38] as does the *N*-terminus of bradykinin potentiating peptides (BPPs) from the crude venom of the viper *Bothrops jararaca* [39]. Biosynthetically, Pyr peptides originate from glutaminyl peptides by the action of pyroglutamyl cyclases. Currently, more than 100 pyroglutamyl cyclase-type genes can be found in genomic databases such as BLAST (Basic Local Alignment Tool, National Center for Biotechnology Information), including fungal sources. Thus, the possibility of the formation of the truncated peptaibols before extraction can also not be generally ruled out at present. Future studies have to be performed in order to unequivocally prove the origin of the truncated Pyr peptaibols by *T. viride*.

Further confirmation of the identity of [desAA(1–6),Pyr^7] ALM F30 (**7**) and [desPheol] ALM F30 (**8**) may be derived from the so-called sigma™ value that represents a calculated parameter based on the true isotopic pattern (TIP™; Bruker Daltonik). It considers

the mass and the relative intensities of all isotopes. For both substances, the calculated elemental composition based on the isotopic pattern of the $[M + 2H]^{2+}$ ion belongs to the top 10% of possible hits.

The microheterogeneous ALM F30 isolated from a fermentation broth has previously been analyzed by HPLC–MS and 10 components have been identified [2]. Except for one compound (peptaibol F30/6 in Ref. 2 corresponding to [Glu^7] ALM F30 (**11**) in this study) all components possess only one chargeable function with Glu in position 19. Further amino acid exchanges reported in [2] include Val to Aib or Leu in position 9, Leu to Val in position 12 and Aib to Val in position 17 besides the exchange of Ala with Aib in position 6, which was also found for the peptaibols described in the present study. Seven of these peptaibols were not identified by NACE–ESI-IT-MS. However, careful analysis of the ESI-TOF-MS runs revealed that the peptaibols with the sequences AcUPUAUAQU**U**UGLUPVUUEQFol (F30/1 in Ref. 2) and AcUPUAUAQUVUG**V**UPVUUEQFol (F30/2 in Ref. 2) apparently comigrate with the major components ALM F30 (**4**) and [Aib^6] ALM F30 (**3**) in NACE. Other peptaibols identified in Ref. 2 have identical masses as the major components or masses differing by only 14 Da. As described above, a mass difference of 14 Da between peptides of approximately 1950 Da may not always be sufficient to be translated into a separation by CE. Thus, it appears very likely that most of the minor peptaibol components described in Ref. 2 comigrate with the major components of ALM F30 in NACE. Owing to the large excess of the major component, it was not possible to properly select the appropriate precursor ions for amino acid sequence elucidation of comigrating minor components by NACE–ESI-MS^n.

In contrast, the majority of minor peptaibol components identified by NACE–MS possesses a second carboxy function due to Gln/Glu exchange or loss of the *C*-terminal Pheol. Except for [Glu^7] ALM F30 (component F30/6 in Ref. 2), these compounds were not detected in the earlier HPLC–MS study. Apparently, ALM F30 peptaibols possessing only one carboxy function are separated more efficiently by HPLC, while components with two carboxy functions can be analyzed better by NACE. This illustrates the complementarity of both techniques due to their different separation principles.

Quantification of ALM F30 Components

The relative amounts of the respective peptaibol peptides in a heterogeneous mixture is required in order to judge the relevance of structural variations of individual peptides, in particular, when bioactivities are discussed. In the present NACE assay, the composition cannot be directly obtained from the electropherograms because of the comigration of compounds. Thus, the amount of the identified ALM F30 components in the microheterogeneous mixture was estimated from the NACE-UV traces at 215 nm in combination with the NACE–ESI-TOF-MS results. The relative amount of comigrating or incompletely separated peptides was calculated on the basis of the corrected peak area (peak area divided by the migration time) obtained from the EIE of characteristic isotopic signals of the pseudomolecular $[M + 2H]^{2+}$ and $[M + 3H]^{3+}$ ions, while the absolute amount of comigrating peptides was calculated from the corrected peak area obtained from the NACE-UV trace. Only peptide fragments with similar charges and masses were chosen for the relative

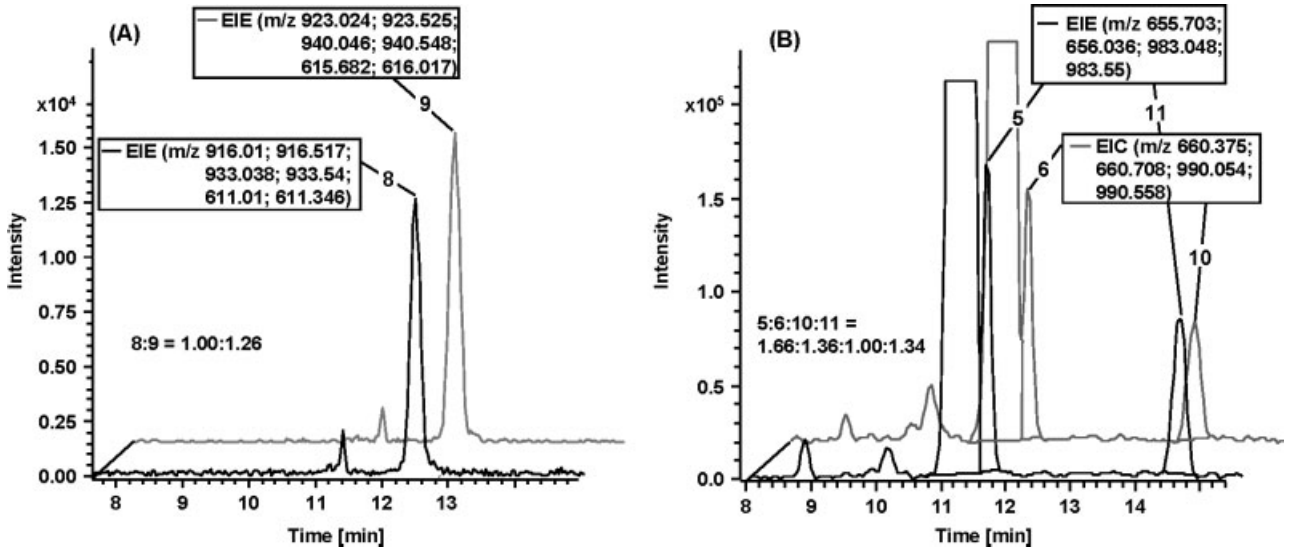

Figure 6 Quantification of (A) [desPheol] ALM F30 (**8**) and [Aib^6,des Pheol], ALM F30 (**9**) and (B) [Glu^{19}] ALM F30 (**5**), [Aib^6,Glu^{19}] ALM F30 (**6**), [Glu^7] ALM F30 (**11**) and [Aib^6,Glu^7] ALM F30 (**10**) by NACE–ESI-TOF-MS. The mass traces shown result from the addition of the unambiguously identified isotope signals of the respective analytes.

quantification, so that comparable ionization yields using ESI can be assumed for the respective analytes. Careful selection of the correct m/z values is important because signal overlapping by ammonium adducts of comigrating peptides occurs. Figure 6A shows the EIE of [desPheol] ALM F30 (**8**) and [Aib^6,desPheol] ALM F30 (**9**). The integration of the peaks resulted in a quantitative relationship of 1.00 : 1.26. The quantification of the other comigrating substances [Glu^{19}] ALM F30 (**5**) and [Aib^6,Glu^{19}] ALM F30 (**6**) as well as [Glu^7] ALM F30 (**11**) and [Aib^6,Glu^7] ALM F30 (**10**) based on the EIE is shown in Figure 6B. Note that the positionally isomeric peptides **5** and **11** form identical pseudomolecular ions as do the positionally isomeric peptides **6** and **10**. The resulting quantitative relationship for these four peptides is 1.66 : 1.36 : 1.00 : 1.34. The relative amount of the pyroglutamyl peptides and of the pair ALM F30 (**4**)/[Aib^6] ALM F30 (**3**) was calculated in a similar manner.

The results of the quantitative analysis are listed in Table 1. In accordance with the results obtained by Brückner and coworkers for ALM F30 using HPLC–MS [2], the main components ALM F30 (**4**) and [Aib^6] ALM F30 (**3**) comprise about 90% of the ALM F30 peptides. The unusual compound [desAA(1–6),Pyr^7] ALM F30 (**7**) was present at a level of about 3% while all other minor components were below 2%. The neutral ALM F50 is transported by the EOF. The quantification of analytes comigrating with the EOF is difficult because of signal quenching by impurities transported by the EOF. Therefore, ALM F50 was not quantified.

CONCLUSIONS

The components of ALM F30 isolated from fermentations of *T. viride* were analyzed by NACE–ESI-IT-MS and NACE–ESI-TOF-MS. A total of 11 compounds were identified. These are characterized by the well-known Ala/Aib exchange in position 6 as well as additional Gln/Glu exchanges in positions 7 or 19, as well as the loss of the *C*-terminal Pheol residue. Additionally, two truncated pyroglutamyl derivatives were detected which have not been described for peptaibols from fungal sources before.

Compared to an earlier study on ALM F30 by HPLC–MS [2], the present results are in agreement with regard to the structure and content of the major components ALM F30 and [Aib^6] ALM F30. However, the discrepancy concerning the minor components is evident. Most of the minor components described in the HPLC study were not detected by NACE–ESI-IT-MS. This may be explained by the fact that the mass differences of $\pm$14 Da between compounds in many cases are not sufficient to translate into a separation in CE. On the other hand, most of the compounds found by NACE–MS were not identified by HPLC–MS. These components are characterized by an additional carboxy group caused by the exchange to Gln *versus* Glu or loss of the *C*-terminal amino alcohol. Apparently, the additional charge makes such compounds more suitable for CE analysis while they were 'missed' by HPLC. This demonstrates that HPLC and CE are complementary techniques due to the different separation mechanisms. For complete characterization of complex peptide mixtures, both techniques should be applied.

Acknowledgements

We are indebted to Dr Harald Bocker (Jena) and Prof. em. Dr Detlef Gröger (Halle/Saale) for valuable discussions on the occurrence of pyroglutamic acid in fungal peptides and microbial sources.

REFERENCES

1. Meyer CE, Reusser F. A polypeptide antibacterial agent isolated from *Trichoderma viride*. *Experienta* 1967; **23**: 85–86.
2. Kirschbaum J, Krause C, Winzheimer RK, Brückner H. Sequences of alamethicins F30 and F50 reconsidered and reconciled. *J. Pept. Sci.* 2003; **9**: 799–809.
3. Duclohier H, Wróblewski H. Voltage-dependent pore formation and antimicrobial activity by alamethicin and analogues. *J. Membr. Biol.* 2001; **184**: 1–12.
4. Boheim G, Hanke W, Jung G. Alamethicin pore formation: voltage dependent flip-flop of α-helix dipoles. *Biophys. Struct. Mech.* 1983; **9**: 181–191.
5. Menestrina G, Voges KP, Jung G, Boheim G. Voltage-dependent channel formation by rods of helical polypeptides. *J. Membr. Biol.* 1986; **93**: 111–132.
6. Jung G, Redemann T, Meder S, Hirsch A, Boheim G. Template-free self-assembling fullerene and lipopeptide conjugates of alamethicin form voltage-dependent ion channels of remarkable stability and activity. *J. Pept. Sci.* 2003; **9**: 784–798.
7. Whitmore L, Chugh JK, Snook CF, Wallace BA. The peptaibol database: a sequence and structure resource. *J. Pept. Sci.* 2003; **9**: 663–665.
8. Degenkolb T, Berg A, Gams W, Schlegel B, Gräfe U. The occurence of peptaibols and structurally related peptaibiotics in fungi and their mass spectrometric identification via diagnostic fragment Ions. *J. Pept. Sci.* 2003; **9**: 666–678.
9. Pandey RC, Cook CJ, Rinehart KL. High resolution and field desorption mass spectrometry studies and revised structures of alamethicins I and II. *J. Am. Chem. Soc.* 1977; **99**: 8469–8483.
10. Schmitt H, Jung G. Total synthesis of the α-helical eicosapeptide antibiotic alamethicin. *Liebigs Ann. Chem.* 1985; 321–344.
11. Riekkola M-L. Recent advances in nonaqueous capillary electrophoresis. *Electrophoresis* 2002; **23**: 3865–3883.
12. Matysik F-M. Special aspects of detection methodology in nonaqueous capillary electrophoresis. *Electrophoresis* 2002; **23**: 400–407.
13. Weinmann W, Maier C, Baumeister K, Przybylski M, Parker CE, Tomer KB. Isolation of hydrophobic lipoproteins in organic solvents by pressure-assisted capillary electrophoresis for subsequent mass spectrometric characterization. *J. Chromatogr.* 1993; **648**: 251–256.
14. Popa TV, Mant CT, Chen Y, Hodges RS. Capillary zone electrophoresis of small α-helical diastereomeric peptide pairs

with anionic ion-pairing reagents. *J. Chromatogr. A* 2004; **1043**: 113–122.
15. Yang Q, Benson LM, Johnson KL, Naylor S. Analysis of lipophilic peptides and therapeutic drugs: on-line-nonaqueous capillary electrophoresis-mass spectrometry. *J. Biochem. Biophys. Methods* 1999; **38**: 103–121.
16. Stutz H. Advances in the analysis of proteins and peptides by capillary electrophoresis with matrix-assisted laser desorption/ionization and electrospray-mass spectrometry detection. *Electrophoresis* 2005; **26**: 1254–1290.
17. Nguyen H-H, Imhof D, Kronen M, Schlegel B, Härtl A, Gräfe U, Gera L, Reissmann S. Synthesis and biological evaluation of analogues of the peptaibol ampullosporin A. *J. Med. Chem.* 2002; **45**: 2781–2787.
18. Carpino LA, Beyermann M, Wenschuh H, Bienert M. Peptide synthesis via amino acid halides. *Acc. Chem. Res.* 1996; **29**: 268–274.
19. Roepstorff P, Fohlmann J. Proposal for a common nomenclature for sequence ions in mass spectra of peptides. *Biomed. Mass Spectrom.* 1984; **11**: 601.
20. Biemann K. Nomenclature for peptide fragment ions (positive ions). *Methods Enzymol.* 1990; **193**: 886–887.
21. Rebuffat S, Goulard C, Bodo B. Antibiotic peptides from *Trichoderma harzianum*: harzianins HC, proline-rich 14-residue peptaibols. *J. Chem. Soc. Perkin Trans. 1* 1995; 1849–1855.
22. Jaworski A, Brückner H. Sequences of polypeptide antibiotics stilboflavins, natural peptaibol libraries of the mold *Stilbella flavipes*. *J. Pept. Sci.* 2001; **7**: 433–447.
23. Jaworski A, Brückner H. Detection of new sequences of peptaibol antibiotics trichotoxins A-40 by on-line liquid chromatography–electrospray ionization mass spectrometry. *J. Chromatogr. A* 1999; **862**: 179–189.
24. Berg A, Grigoriev PA, Degenkolb T, Neuhof T, Härtl A, Schlegel B, Gräfe U. Isolation, structure elucidation and biological activities of trichofumins A, B, C and D, new 11 and 13mer peptaibols from *Trichoderma* sp. HKI 0276. *J. Pept. Sci.* 2003; **9**: 810–816.
25. Sharman GJ, Try AC, Williams DH, Ainsworth AM, Beneyto R, Gibson TM, McNicholas C, Renno DV, Robinson N, Wood KA, Wrigley SK. Structural elucidation of XR586, a peptaibol-like antibiotic from *Acremonium persicium*. *Biochem. J.* 1986; **320**: 723–728.
26. Brückner H, Kripp M, Kieß M. Polypeptide antibiotics trichovirin and trichobrachin: sequence determination and total synthesis. *Chem. Pept. Proteins* 1993; **5/6**: 357–373.
27. Heinze S, Ritzau M, Ihn W, Schlegel B, Dornberger K, Fleck WF, Zerlin M, Christner C, Gräfe U, Küllertz G, Fischer G. Lipohexin, a new inhibitor of prolyl endopeptidase from *Moeszia lindtneri* (HKI-0096) and *Paecilomyces sp.* (HKI-0055; HKI-0096). I. Screening, isolation and structure elucidation. *J. Antibiotics* 1997; **50**: 379–383.
28. Christner C, Zerlin M, Gräfe U, Heinze S, Küllertz G, Fischer G. Lipohexin, a new inhibitor of prolyl endopeptidase from *Moeszia lindtneri* (HKI-0054) and *Paecilomyces sp.* (HKI-0055; HKI-0096). II. Inhibition activity and specificity. *J. Antibiotics* 1997; **50**: 384–389.
29. Rebuffat S, Goulard C, Hlimi S, Bodo B. Two unprecedented natural Aib-peptides with the (Xaa-Yaa-Aib-Pro) motif and an unusual C-terminus: Structures. Membrane modifying and antibacterial properties of pseudokinins KL III and KL VI from the fungus *Trichoderma pseudokoningii*. *J. Pept. Sci.* 2000; **6**: 519–533.
30. Schiell M, Hofmann J, Kurz M, Schmidt FR, Vertesy L, Vogel M, Wink J, Seibert G. Cephaibols, new peptaibol antibiotics with antihelmintic properties from *Acremonium tubakii* DSM 12774. *J. Antibiotics* 2001; **54**: 220–233.
31. Mucchetti G, Locci F, Gatti M, Neviani E, Addeo F, Dossena A, Marchelli R. Pyroglutamic acid in cheese: Presence, origin, and correlation with ripening time of grana padano cheese. *J. Dairy Sci.* 2000; **83**: 659–665.
32. Mucchetti G, Locci F, Massara P, Vitale R, Neviani E. Production of pyroglutamic acid by thermophilic lactic acid bacteria in hard-cooked mini-cheeses. *J. Dairy Sci.* 2002; **85**: 2489–2496.
33. Huang R-H, Xiang Y, Liu X-Z, Zhang Y, Hu Z, Wang D-C. Two novel antifungal peptides distinct with a five-disulfide motif from the bark of *Eucommia ulmoides* Oliv. *FEBS Lett.* 2002; **521**: 87–90.
34. Köllisch GV, Lorenz MW, Kellner R, Verhaert PD, Hoffmann KH. Structure elucidation and biological activity of an unusual adipokinetic hormone from corpora cardiaca of the butterfly, *Vanessa cardui*. *Eur. J. Biochem.* 2000; **267**: 5502–5508.
35. Silva PI, Daffre S, Bulet P. Isolation and characterization of gomesin, an 18-residue cysteine-rich defense peptide from the spider *Acanthoscurria gomesiana* hemocytes with sequence similarities to horseshoe crab antimicrobial peptides of the tachylepsin family. *J. Biol. Chem.* 2000; **275**: 33 464–33 470.
36. Garden RW, Moroz TP, Gleeson JM, Floyd PD, Li L, Rubakhin SS, Sweedler J. Formation of N-pyroglutamyl peptides from N-Glu and N-Gln precursors in *Aplysia* neurons. *J. Neurochem.* 1999; **72**: 676–681.
37. Destoumieux D, Bulet P, Loew D, Dorsselaer AV, Rodriguez J, Bachère E. Penaeidins, a new family of antimicrobial peptides isolated from the shrimp *Penaeus vannamei* (Decapoda). *J. Biol. Chem.* 1997; **272**: 28 398–28 406.
38. Desrues L, Tonon M-C, Leprince J, Vaudry H, Conlon JM. Isolation, primary structure, and effects on α-melanocyte-stimulating hormone release of frog neurotensin. *Endocrinology* 1998; **139**: 4140–4146.
39. Ianzer D, Konno K, Marques-Porto R, Portaro FCV, Stöcklin R, de Camargo ACM, Pimenta DC. Identification of five new bradykinin potentiating peptides (BPPs) from *Bothrops jararaca* crude venom by using electrospray ionization tandem mass spectrometry after a two-step liquid chromatography. *Peptides* 2004; **25**: 1085–1092.

